



The Compact Muon Solenoid Experiment

CMS Note

Mailing address: CMS CERN, CH-1211 GENEVA 23, Switzerland



January 25, 2013

Searches for beyond-the-standard model physics in events with a Z boson, jets and missing transverse energy

D. Barge, C. Campagnari, D. Kovalskyi, V. Krutelyov

University of California, Santa Barbara, USA

W. Andrews, G. Cerati, D. Evans, F. Golf, I. MacNeill, S. Padhi, V. Welke, Y. Tu, F. Würthwein, A. Yagil, J. Yoo

University of California, San Diego, USA

L. Bauerdick, K. Burkett, I. Fisk, Y. Gao, O. Gutsche, B. Hooberman, S. Jindariani, J. Linacre, V. Martinez
Otschoorn

Fermi National Accelerator Laboratory, Batavia, Illinois, USA

Abstract

This note describes a search for beyond-the-standard model (BSM) physics in events with a leptonically-decaying Z boson, jets, and missing transverse energy (E_T^{miss}). This signature is predicted to occur in several BSM scenarios, for example supersymmetric (SUSY) models. Two search strategies are pursued. The first is an inclusive approach which selects events with at least two jets and large E_T^{miss} , produced in association with the $Z \rightarrow \ell\ell$ candidate. The second is a targeted search in which additional requirements are imposed in order to achieve sensitivity to the production of the weakly-coupled SUSY charginos and neutralinos. The main backgrounds of SM $Z + \text{jets}$ and $t\bar{t}$ production are estimated with the data-driven E_T^{miss} templates technique and the opposite-flavor subtraction technique, respectively. Additional backgrounds are estimated from simulation, after validation in data control samples. In both the inclusive and targeted analyses, good agreement is observed between the data and predicted background over the full E_T^{miss} range. The results are interpreted in the context of a simplified SUSY model, and used to place constraints on the masses of the electroweak charginos and neutralinos.

Contents

1	Changes w.r.t. previous AN Version	3
2	Introduction	3
3	Datasets and Triggers	5
4	Selection	6
4.1	Event Selection	6
4.2	Lepton Selection	6
4.2.1	Electron Selection	6
4.2.2	Muon Selection	6
4.3	Photons	6
4.4	MET	7
4.5	Jets	7
5	Data vs. MC Comparison in Preselection Region	8
6	Background Estimation Techniques	11
6.1	Estimating the Z + jets Background with E_T^{miss} Templates	11
6.2	Estimating the Flavor-Symmetric Background with $e\mu$ Events	12
6.3	Estimating the WZ and ZZ Background with MC	14
6.3.1	WZ Validation Studies	14
6.3.2	ZZ Validation Studies	16
7	Results	17
8	Summary	19
A	Results in the ee and $\mu\mu$ Channels	21
B	E_T^{miss} Templates from γ + jets Sample	25

1 Changes w.r.t. previous AN Version

- v7: Add rejection of PU jets using the beta variable. Update the trigger efficiencies using measurements of the full 2012 sample. Update the data sample to the full 19.5 fb^{-1} . Correct the cross sections for the ZZZ and ZZJetsTo2L2Q MC samples.
- v6: Updated experimental results based on full 2012 sample, corresponding to 19.3 fb^{-1} .
- v5: **This is the version corresponding to the HCP results.** Added interpretation for the GMSB model. Added data vs. MC kinematic distributions for the sample with 3 leptons and at least 2 jets, where we observe an excess of data with respect to the MC prediction.
- v4: Un-blinded the results of the inclusive and targeted analysis, and added an interpretation in the WZ + E_T^{miss} model. Moved the material for the edge analysis to a separate AN (2012/359).
- v3: Added results for the low- E_T^{miss} and high- E_T^{miss} signal regions used for the edge analysis, for the first 5.1 fb^{-1} 2012A+B data.
- v2: Updated to 9.2 fb^{-1} of 53X data and MC (v1 used 5.1 fb^{-1} 52X data and MC).

2 Introduction

This note presents two searches for beyond-the-standard model (BSM) physics in events containing a leptonically-decaying Z boson, jets, and missing transverse energy. This is an update of previous searches performed with 2011 data [1, 2]. The search is based on a data sample of pp collisions collected at $\sqrt{s} = 8 \text{ TeV}$ in 2012, corresponding to an integrated luminosity of 19.5 fb^{-1} .

The production of Z bosons is expected in many BSM scenarios, for example supersymmetric (SUSY) models. In SUSY models with neutralino lightest SUSY particle (LSP), Z bosons may be produced in the decays $\chi_2^0 \rightarrow Z\chi_1^0$, where χ_2^0 is the second lightest neutralino and χ_1^0 is the lightest neutralino. In models with gravitino LSP such as gauge-mediated SUSY breaking (GMSB) models, Z bosons may be produced via $\chi_1^0 \rightarrow Z\tilde{G}$, where \tilde{G} is the gravitino. Such decays may occur either in the cascade decays of the strongly-produced squarks and gluinos, or via direct production of the electroweak charginos and neutralino. Examples of such processes (see Fig. 1) are:

- strong production: $pp \rightarrow \tilde{g}\tilde{g} \rightarrow (q\bar{q}\chi_2^0)(q\bar{q}\chi_2^0) \rightarrow (q\bar{q}Z\chi_1^0)(q\bar{q}Z\chi_1^0) \rightarrow ZZ + 4 \text{ jets} + E_T^{\text{miss}}$
- electroweak production: $pp \rightarrow \chi_1^\pm \chi_2^0 \rightarrow (W\chi_1^0)(Z\chi_1^0) \rightarrow WZ + E_T^{\text{miss}}$

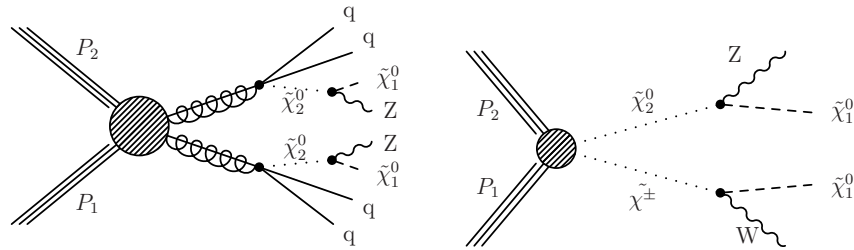


Figure 1: Examples of BSM physics signatures targeted in this search. In the left diagram, Z bosons are produced in the cascade decays of the strongly-interacting gluinos. In the right diagram, a Z boson is produced via direct production of the weakly-coupled charginos and neutralinos.

We thus pursue two strategies. The first is an inclusive strategy which selects events with a $Z \rightarrow \ell\ell$ candidate, at least two jets, and large E_T^{miss} . This strategy is useful for targeting, e.g., the production of Z bosons in the cascade decays of strongly-interacting particles as depicted in Fig. 1 (left). In the second strategy, we impose additional requirements which strongly suppress the backgrounds while retaining high efficiency for events with Z bosons produced via direct production of the weakly-coupled charginos and neutralinos. These two strategies are referred to as the “inclusive search” and the “targeted search,” respectively.

After selecting events with jets and a $Z \rightarrow \ell^+\ell^-$ ($\ell = e, \mu$) candidate, the dominant background consists of SM Z production accompanied by jets from initial-state radiation (Z + jets). The E_T^{miss} in Z + jets events arises

35 primarily when jet energies are mismeasured. The $Z + \text{jets}$ cross section is several orders of magnitude larger
 36 than our signal, and the artificial E_T^{miss} is not necessarily well reproduced in simulation. Therefore, the critical
 37 prerequisite to a discovery of BSM physics in the $Z + \text{jets} + E_T^{\text{miss}}$ final state is to establish that a potential excess
 38 is not due to SM $Z + \text{jets}$ production accompanied by artificial E_T^{miss} from jet mismeasurements. In this note,
 39 the $Z + \text{jets}$ background is estimated with the E_T^{miss} templates technique, in which the artificial E_T^{miss} in $Z + \text{jets}$
 40 events is modeled using a $\gamma + \text{jets}$ control sample. The second background category consists of processes which
 41 produce leptons with uncorrelated flavor. These “flavor-symmetric” (FS) backgrounds, which are dominated by $t\bar{t}$
 42 but also contain WW , $DY \rightarrow \tau\tau$ and single top processes, are estimated using a data control sample of $e\mu$ events.
 43 Additional backgrounds from WZ and ZZ production are estimated from MC, after validation of the MC modeling
 44 of these processes using 3-lepton and 4-lepton data control samples.

3 Datasets and Triggers

In this section we list the datasets, triggers, and MC samples used in the analysis. For selecting signal events, we use dilepton triggers in the DoubleElectron, DoubleMu, and MuEG datasets. An event in the ee final state is required to pass the dielectron trigger, a $\mu\mu$ event is required to pass the dimuon trigger, while an $e\mu$ event is required to pass at least one of the two $e - \mu$ cross triggers. The efficiencies of the ee and $e\mu$ triggers with respect to the offline selection with two $p_T > 20$ GeV have been measured as 0.95 ± 0.03 , 0.93 ± 0.03 , respectively. The $\mu\mu$ trigger efficiency is 0.90 ± 0.03 for events with two muons satisfying $|\eta| < 1$, and 0.81 ± 0.03 otherwise (the average trigger efficiency is 0.86 ± 0.03). A sample of $\gamma + \text{jets}$ events, used as a control sample to estimate the $Z + \text{jets}$ background, is selected using a set of single photon triggers. The golden prompt reco json and rereco jsons are merged, yielding an integrated luminosity of 19.5 fb^{-1} .

- Datasets

- DoubleElectron
- DoubleMu
- MuEG

- Datasets

- Run2012A-13Jul2012-v1
- Run2012A-recover-06Aug2012-v1
- Run2012B-13Jul2012-v1
- Run2012C-24Aug2012-v1
- Run2012C-PromptReco-v2
- MuEG_Run2012D-PromptReco-v1

- Triggers

- HLT_Mu17_Mu8_v*
- HLT_Mu17_Ele8_CaloIdT_CaloIsoVL_TrkIdVL_TrkIsoVL_v*
- HLT_Mu8_Ele17_CaloIdT_CaloIsoVL_TrkIdVL_TrkIsoVL*
- HLT_Ele17_CaloIdT_CaloIsoVL_TrkIdVL_TrkIsoVL_Ele8_CaloIdT_CaloIsoVL_TrkIdVL_TrkIsoVL_v*
- HLT_Photon22_R9Id90_HE10_Iso40_EBOnly_v*
- HLT_Photon36_R9Id90_HE10_Iso40_EBOnly_v*
- HLT_Photon50_R9Id90_HE10_Iso40_EBOnly_v*
- HLT_Photon75_R9Id90_HE10_Iso40_EBOnly_v*
- HLT_Photon90_R9Id90_HE10_Iso40_EBOnly_v*

Table 1: List of MC samples.

Process	Dataset Name	Cross Section [pb]
$Z + \text{jets}$	/DYJetsToLL_M-50_TuneZ2star_8TeV-madgraph-tarball/Summer12_DR53X-PU_S10_START53_V7A-v1/AODSIM	3532.8
$t\bar{t}$	/TTJets_MassiveBinDECAY_TuneZ2star_8TeV-madgraph-tauola/Summer12_DR53X-PU_S10_START53_V7A-v1/AODSIM	225.2
ZZ	/ZZJetsTo4L_TuneZ2star_8TeV-madgraph-tauola/Summer12_DR53X-PU_S10_START53_V7A-v1/AODSIM	0.1769
	/ZZJetsTo2L2Q_TuneZ2star_8TeV-madgraph-tauola/Summer12_DR53X-PU_S10_START53_V7A-v1/AODSIM	2.4487
	/ZZJetsTo2L2Nu_TuneZ2star_8TeV-madgraph-tauola/Summer12_DR53X-PU_S10_START53_V7A-v3/AODSIM	0.3648
WZ	/WZJetsTo3LNu_TuneZ2star_8TeV-madgraph-tauola/Summer12_DR53X-PU_S10_START53_V7A-v1/AODSIM	1.0575
	/WZJetsTo2L2Q_TuneZ2star_8TeV-madgraph-tauola/Summer12_DR53X-PU_S10_START53_V7A-v1/AODSIM	2.206
WW	/WWJetsTo2L2Nu_TuneZ2star_8TeV-madgraph-tauola/Summer12_DR53X-PU_S10_START53_V7A-v1/AODSIM	5.8123
single top	/T_tW-channel-DR_TuneZ2star_8TeV-powheg-tauola/Summer12_DR53X-PU_S10_START53_V7A-v1/AODSIM	11.177
	/Tbar_tW-channel-DR_TuneZ2star_8TeV-powheg-tauola/Summer12_DR53X-PU_S10_START53_V7A-v1/AODSIM	11.177
$t\bar{t}V$	/TTZJets_8TeV-madgraph_v2/Summer12_DR53X-PU_S10_START53_V7A-v1/AODSIM	0.208
	/TTWJets_8TeV-madgraph/Summer12_DR53X-PU_S10_START53_V7A-v1/AODSIM	0.232
VVV	/ZZZNoGstarJets_8TeV-madgraph/Summer12_DR53X-PU_S10_START53_V7A-v1/AODSIM	0.0055
	/WWWJets_8TeV-madgraph/Summer12_DR53X-PU_S10_START53_V7A-v1/AODSIM	0.08217
	/WWZNoGstarJets_8TeV-madgraph/Summer12_DR53X-PU_S10_START53_V7A-v1/AODSIM	0.0633
	/WZZNoGstarJets_8TeV-madgraph/Summer12_DR53X-PU_S10_START53_V7A-v1/AODSIM	0.01922

4 Selection

In this section, we list the event selection, electron and muon objects selections, jets, E_T^{miss} , and b-tagging selections used in this analysis. These selections are based on those recommended by the relevant POG's.

4.1 Event Selection

We require the presence of at least one primary vertex satisfying the standard quality criteria; namely, vertex is not fake, $\text{ndf} \geq 4$, $\rho < 2$ cm, and $|z| < 24$ cm.

4.2 Lepton Selection

Because $Z \rightarrow \ell\ell$ ($\ell = e, \mu$) is a final state with very little background, we restrict ourselves to events in which the Z boson decays to electrons or muons only. Therefore opposite sign leptons passing the identification and isolation requirements described below are required in each event.

- $p_T > 20$ GeV and $|\eta| < 2.4$;
- Opposite-sign same-flavor (SF) ee and $\mu\mu$ lepton pairs (opposite-flavor (OF) $e\mu$ lepton pairs are retained in a control sample used to estimate the FS contribution);
- For SF events, the dilepton invariant mass is required to be consistent with the Z mass; namely $81 < m_{\ell\ell} < 101$ GeV.

4.2.1 Electron Selection

The electron selection is the loose working point recommended by the E/gamma POG, as documented at [3]. Electrons with $p_T > 20$ GeV and $|\eta| < 2.4$ are considered. We use PF-based isolation with a cone size of $\Delta R < 0.3$, using the effective area rho corrections documented at [4], and we require a relative isolation < 0.15 . Electrons in the transition region defined by $1.4442 < |\eta_{SC}| < 1.566$ are rejected. Electrons with a selected muon with $p_T > 10$ GeV within $\Delta R < 0.1$ are rejected. The electron selection requirements are listed in Table 2 for completeness.

Table 2: Summary of the electron selection requirements.

Quantity	Barrel	Endcap
$\delta\eta$	< 0.007	< 0.009
$\delta\phi$	< 0.15	< 0.10
$\sigma_{i\eta i\eta}$	< 0.01	< 0.03
H/E	< 0.12	< 0.10
d_0 (w.r.t. 1st good PV)	< 0.02 cm	< 0.02 cm
d_z (w.r.t. 1st good PV)	< 0.2 cm	< 0.2 cm
$ 1/E - 1/P $	$< 0.05 \text{ GeV}^{-1}$	$< 0.05 \text{ GeV}^{-1}$
PF isolation / p_T	< 0.15	< 0.15
conversion rejection: fit probability	$< 10^{-6}$	$< 10^{-6}$
conversion rejection: missing hits	≤ 1	≤ 1

4.2.2 Muon Selection

We use the tight muon selection recommended by the muon POG, as documented at [5]. Muons with $p_T > 20$ GeV and $|\eta| < 2.4$ are considered. We use PF-based isolation with a cone size of $\Delta R < 0.3$, using the $\Delta\beta$ PU correction scheme, and we require a relative isolation of < 0.15 . The muon selection requirements are listed in Table 3 for completeness.

4.3 Photons

As will be explained later, it is not essential that we select real photons. What is needed are jets that are predominantly electromagnetic, well measured in the ECAL, and hence less likely to contribute to fake MET. We select photons with:

Table 3: Summary of the muons selection requirements.

Quantity	Requirement
muon type	global muon and PF muon
χ^2/ndf	< 10
muon chamber hits	≥ 1
matched stations	≥ 2
d_0 (w.r.t. 1st good PV)	$< 0.02 \text{ cm}$
d_z (w.r.t. 1st good PV)	$< 0.5 \text{ cm}$
pixel hits	≥ 1
tracker layers	≥ 5

- $p_T > 22 \text{ GeV}$
- $|\eta| < 2$
- $H/E < 0.1$
- No matching pixel track (pixel veto)
- There must be a pfjet of $p_T > 10 \text{ GeV}$ matched to the photon within $dR < 0.3$. The matched jet is required to have a neutral electromagnetic energy fraction of at least 70%.
- We require that the pfjet p_T matched to the photon satisfy (pfjet p_T - photon p_T) $> -5 \text{ GeV}$. This removes a few rare cases in which “overcleaning” of a pfjet generates fake MET.
- We also match photons to calojets and require (calojet p_T - photon p_T) $> -5 \text{ GeV}$ (the same requirement used for pfjets). This is to remove other rare cases in which fake energy is added to the photon object but not the calojet.
- We reject photons which have an electron of at least $p_T > 10 \text{ GeV}$ within $dR < 0.2$ in order to reject conversions from electrons from W decays which are accompanied by real MET.
- We reject photons which are aligned with the MET to within 0.14 radians in phi.

4.4 MET

We use pfmet, henceforth referred to simply as E_T^{miss} .

4.5 Jets

- PF jets with L1FastL2L3 corrections (MC), L1FastL2L3residual corrections (data), using the 52X jet energy corrections
- $|\eta| < 2.5$
- Passes loose PFJet ID
- $p_T > 30 \text{ GeV}$ for determining the jet multiplicity, $p_T > 15 \text{ GeV}$ for calculation of H_T
- For the creation of photon templates, the jet matched to the photon passing the photon selection described above is vetoed
- For the dilepton sample, jets are vetoed if they are within $\Delta R < 0.4$ from any lepton $p_T > 20 \text{ GeV}$ passing analysis selection
- To reject PU jets, we require the jets to satisfy $\beta > 0.2$, defined for each jet using the d_Z of the tracks in the jet with respect to the primary vertex. To calculate β we take the sum of the p_T^2 of the tracks associated to PFCandidates in the jet that are consistent with originating from the primary vertex ($d_Z < 0.5 \text{ cm}$), and divide by the sum p_T^2 of all the tracks:

$$\beta = \frac{\sum_i^{d_z < 0.5 \text{ cm}} (p_T^i)^2}{\sum_i^{\text{all}} (p_T^i)^2} \quad (1)$$

5 Data vs. MC Comparison in Preselection Region

In this section we compare the data and MC samples passing the selection described in Sec. 4. In the following, the MC is reweighted to match the data distribution of number of reconstructed primary vertices. The trigger efficiencies of Sec. 3 are applied. In all plots, the last bin contains the overflow.

We begin by counting the inclusive Z yields. Here we require the presence of two selected leptons without any additional requirements on jets or E_T^{miss} . In Fig. 2 the distribution of dilepton invariant mass in the ee and $\mu\mu$ channels is displayed. In Table 4 the yields for selected dilepton events in the Z mass window are indicated. Good data vs. MC agreement is observed, within the systematic uncertainties of integrated luminosity (4.5%), trigger efficiency (3%), Z + jets and $t\bar{t}$ cross sections.

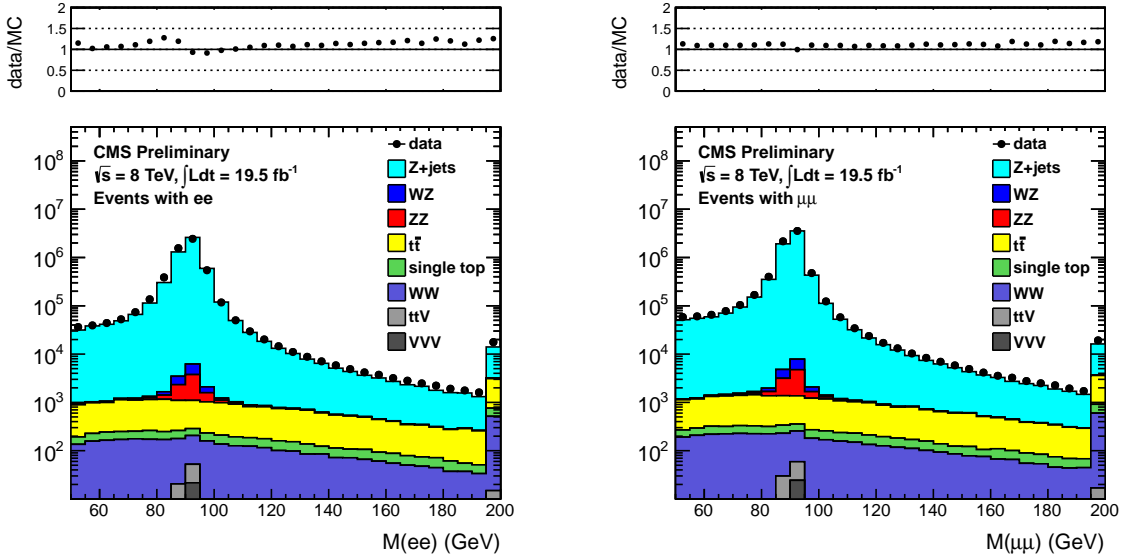


Figure 2: Dilepton mass distribution for events with two selected leptons in the ee (left) and $\mu\mu$ (right) final states.

Table 4: Data and Monte Carlo yields for events with two selected leptons in the Z mass window.

Sample	ee	$\mu\mu$	$e\mu$	total
Z + jets	4776593 ± 3391	6227613 ± 3627	2328 ± 73.9	11006533 ± 4966
$t\bar{t}$	3321.1 ± 45.8	4014.4 ± 47.6	7621.3 ± 68.7	14956.8 ± 95.3
WW	614.8 ± 6.0	773.7 ± 6.3	1433.1 ± 9.0	2821.7 ± 12.6
WZ	4342.7 ± 7.3	5411.7 ± 7.7	115.3 ± 1.1	9869.7 ± 10.6
ZZ	4712.8 ± 9.9	5906.1 ± 10.5	21.0 ± 0.3	10639.8 ± 14.4
single top	315.3 ± 11.9	388.4 ± 12.4	709.5 ± 17.6	1413.2 ± 24.6
$t\bar{t}V$	57.4 ± 1.1	68.1 ± 1.1	21.8 ± 0.7	147.3 ± 1.7
VVV	30.1 ± 0.3	36.4 ± 0.4	6.9 ± 0.2	73.5 ± 0.5
total SM MC	4789987.0 ± 3391.1	6244211.0 ± 3627.1	12256.7 ± 102.8	11046454.7 ± 4966.5
data	4906970	6552612	13141	11472723

We next define the preselection region for the inclusive search using the following requirements:

- Number of jets ≥ 2 ;
- Same flavor dileptons (opposite flavor yields will be shown since they are used in data for the FS background estimation);
- Dilepton invariant mass $81 < m_{\ell\ell} < 101$ GeV.

The dilepton mass distributions in the preselection region of the inclusive search (without the dilepton mass requirement applied) for the ee and $\mu\mu$ final states are shown in Figure 3. In Table 5 the data and MC yields in the inclusive preselection region are indicated. Good data vs. MC agreement is observed.

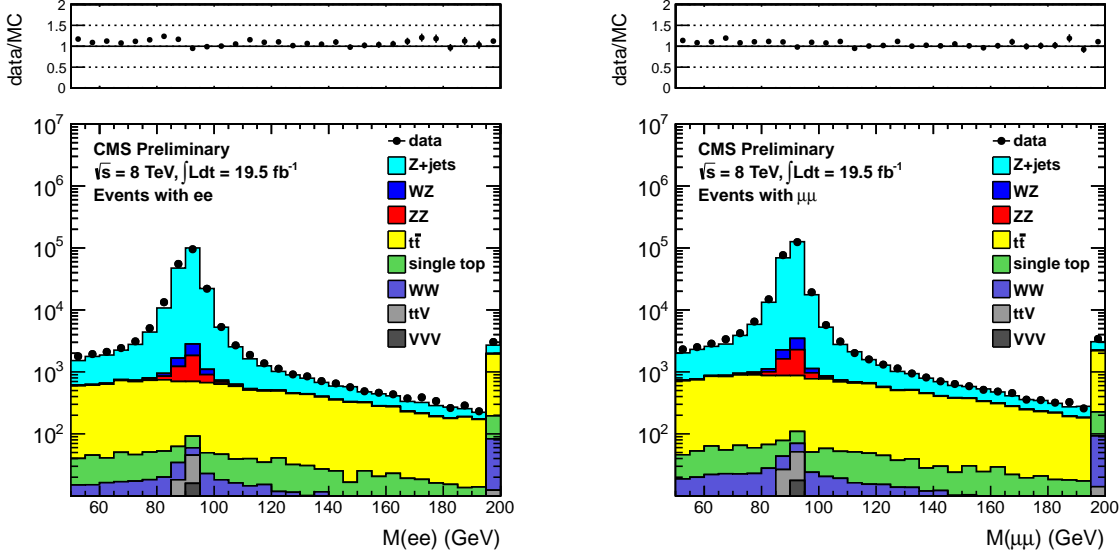


Figure 3: Dilepton mass distribution for events in the preselection region of the inclusive search in the ee (left) and $\mu\mu$ (right) final states.

Table 5: Data and MC yields in the preselection region of the inclusive search.

Sample	ee	$\mu\mu$	$e\mu$	total
Z + jets	174022.4 ± 645.0	218277.0 ± 678.9	86.9 ± 14.4	392386.4 ± 936.5
$t\bar{t}$	2536.3 ± 40.1	3058.7 ± 41.6	5824.7 ± 60.1	11419.7 ± 83.3
WW	59.5 ± 1.9	73.2 ± 1.9	134.2 ± 2.8	266.9 ± 3.9
WZ	1709.7 ± 4.7	2098.1 ± 4.9	20.0 ± 0.4	3827.8 ± 6.8
ZZ	2002.4 ± 6.9	2477.2 ± 7.2	4.2 ± 0.2	4483.8 ± 9.9
single top	121.2 ± 7.4	137.7 ± 7.4	263.7 ± 10.7	522.6 ± 15.0
$t\bar{t}V$	54.9 ± 1.0	65.6 ± 1.1	20.0 ± 0.6	140.5 ± 1.6
VVV	21.7 ± 0.3	26.2 ± 0.3	3.4 ± 0.1	51.3 ± 0.4
total SM MC	180528.1 ± 646.4	226213.8 ± 680.2	6357.1 ± 62.7	413098.9 ± 940.4
data	185555	234132	6231	425918

We next define the preselection region for the targeted search by adding the following requirements:

- Veto events containing a b-tagged jet;
- Dijet invariant mass $70 < m_{jj} < 110$ GeV;
- Veto events containing a third selected lepton (electron or muon) with $p_T > 10$ GeV;

The rejection of events with a b-tagged jet strongly suppresses the $t\bar{t}$ background, which is the dominant background in the inclusive search after requiring large E_T^{miss} . The requirement that the jet pair is consistent with originating from W/Z decay is motivated by the fact that we are searching for signatures producing $V(\text{jj})Z(\ell\ell)+E_T^{\text{miss}}$; this requirement suppresses the $Z + \text{jets}$ and $t\bar{t}$ backgrounds. The veto of events containing a third electron or muon suppresses the WZ background, and also serves to make this analysis exclusive with respect to searches in the trilepton final state.

The dilepton mass distributions in the preselection region of the targeted search (without the dilepton mass requirement applied) for the ee and $\mu\mu$ final states are shown in Figure 4. In Table 6 the data and MC yields in the preselection region are indicated. Good data vs. MC agreement is observed. We also show the distribution of dijet mass in the targeted preselection (with the requirement on this quantity removed) in Fig. 5, which demonstrates that the MC does a reasonable job of modeling this quantity.

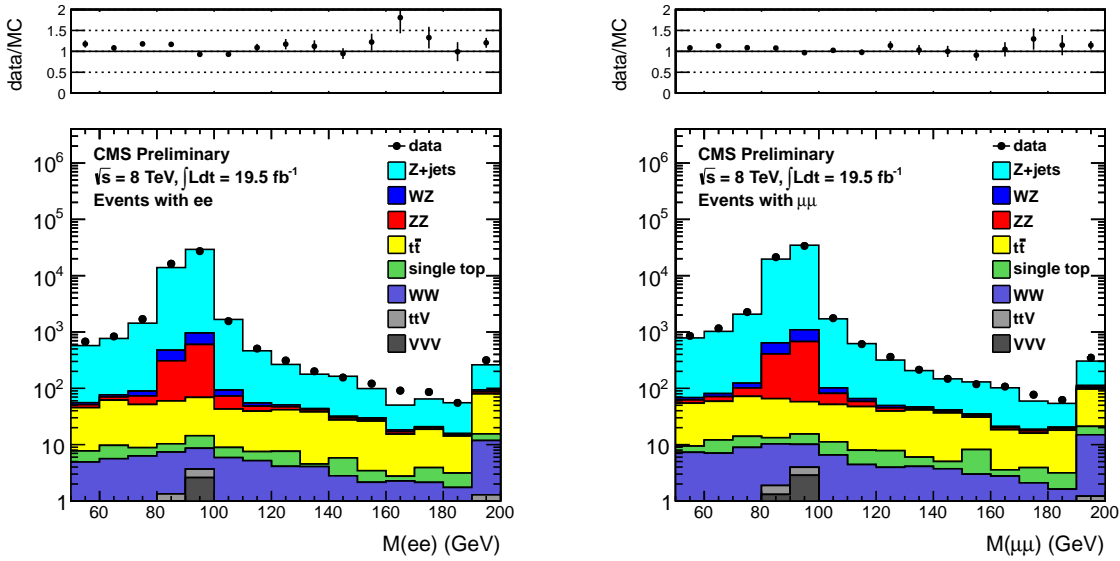


Figure 4: Dilepton mass distribution for events in the preselection region of the targeted search in the ee (left) and $\mu\mu$ (right) final states.

Table 6: Data and MC yields in the preselection region of the targeted search.

Sample	ee	$\mu\mu$	$e\mu$	total
Z + jets	41811.7 ± 316.2	52620.2 ± 333.3	19.4 ± 6.9	94451.2 ± 459.4
$t\bar{t}$	99.9 ± 8.0	95.8 ± 7.3	215.1 ± 11.5	410.8 ± 15.8
WW	11.0 ± 0.8	14.1 ± 0.8	25.8 ± 1.2	50.9 ± 1.7
WZ	525.4 ± 2.6	648.5 ± 2.7	3.1 ± 0.2	1177.0 ± 3.8
ZZ	779.2 ± 4.3	957.9 ± 4.5	0.8 ± 0.1	1737.9 ± 6.3
single top	9.1 ± 2.1	8.7 ± 1.8	14.0 ± 2.4	31.9 ± 3.7
$t\bar{t}V$	1.6 ± 0.2	1.7 ± 0.2	0.8 ± 0.1	4.1 ± 0.3
VVV	3.4 ± 0.1	4.2 ± 0.1	0.9 ± 0.1	8.5 ± 0.2
total SM MC	43241.2 ± 316.3	54351.0 ± 333.4	280.0 ± 13.7	97872.2 ± 459.8
data	43444	54851	275	98570

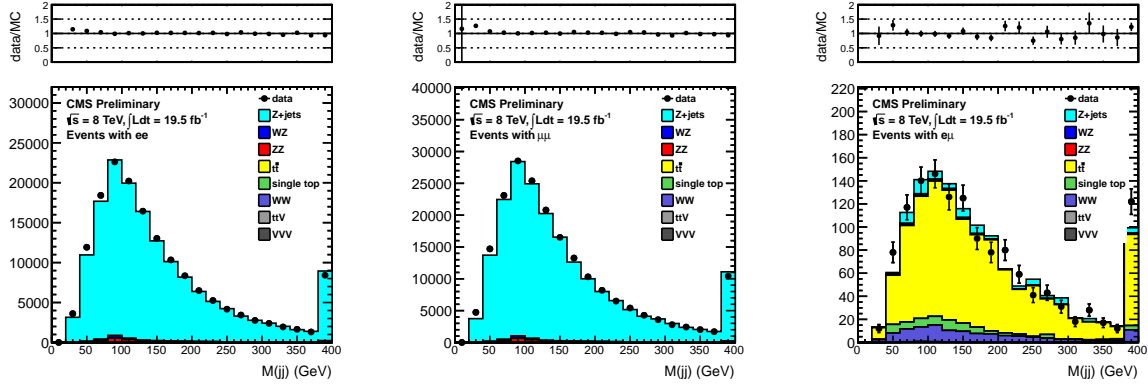


Figure 5: Distributions of dijet mass for the targeted preselection in the ee (left), $\mu\mu$ (middle) and $e\mu$ (right) final state.

6 Background Estimation Techniques

In this section we describe the techniques used to estimate the SM backgrounds in our signal regions defined by requirements of large E_T^{miss} . The SM backgrounds fall into three categories:

- **Z + jets** : this is the dominant background after the preselection. The E_T^{miss} in Z + jets events is estimated with the “ E_T^{miss} templates” technique described in Sec. 6.1;
- **Flavor-symmetric (FS) backgrounds**: this category includes processes which produces 2 leptons of uncorrelated flavor. It is dominated by $t\bar{t}$ but also contains $Z \rightarrow \tau\tau$, WW, and single top processes. This is the dominant contribution in the signal regions, and it is estimated using a data control sample of $e\mu$ events as described in Sec. 6.2;
- **WZ and ZZ backgrounds**: this background is estimated from MC, after validating the MC modeling of these processes using data control samples with jets and exactly 3 leptons (WZ control sample) and exactly 4 leptons (ZZ control sample) as described in Sec. 6.3;

6.1 Estimating the Z + jets Background with E_T^{miss} Templates

The premise of this data driven technique is that E_T^{miss} in Z + jets events is produced by the hadronic recoil system and *not* by the leptons making up the Z. Therefore, the basic idea of the E_T^{miss} template method is to measure the E_T^{miss} distribution in a control sample which has no true MET and the same general attributes regarding fake MET as in Z + jets events. We thus use a sample of γ + jets events, since both Z + jets and γ + jets events consist of a well-measured object recoiling against hadronic jets.

For selecting photon-like objects, the very loose photon selection described in Sec. 4.3 is used. It is not essential for the photon sample to have high purity. For our purposes, selecting jets with predominantly electromagnetic energy deposition in a good fiducial volume suffices to ensure that they are well measured and do not contribute to fake E_T^{miss} . The γ + jets events are selected with a suite of single photon triggers with p_T thresholds varying from 22–90 GeV. The events are weighted by the trigger prescale such that γ + jets events evenly sample the conditions over the full period of data taking. There remains a small difference in the PU conditions in the γ + jets vs. Z + jets samples due to the different dependencies of the γ vs. Z isolation efficiencies on PU. To account for this, we reweight the γ + jets samples to match the distribution of reconstructed primary vertices in the Z + jets sample.

To account for kinematic differences between the hadronic systems in the control vs. signal samples, we measure the E_T^{miss} distributions in the γ + jets sample in bins of the number of jets and the scalar sum of jet transverse energies (H_T). These E_T^{miss} templates are extracted separately from the 5 single photon triggers with thresholds 22, 36, 50, 75, and 90 GeV, so that the templates are effectively binned in photon p_T . All E_T^{miss} distributions are normalized to unit area to form “MET templates”. The prediction of the MET in each Z event is the template which corresponds to the N_{jets} , H_T , and Z p_T in the Z + jets event. The prediction for the Z sample is simply the sum of all such templates. All templates are displayed in App. B.

After preselection, there is a small contribution from backgrounds other than $Z + \text{jets}$. To correct for this, the E_T^{miss} templates prediction is scaled such that the total background prediction matches the observed data yield in the E_T^{miss} 0–60 GeV region. Because the non- $Z + \text{jets}$ impurity in the low E_T^{miss} region after preselection is very small, this results in scaling factors of 0.985 (0.995) for the inclusive (targeted) search.

6.2 Estimating the Flavor-Symmetric Background with $e\mu$ Events

In this subsection we describe the background estimate for the FS background. Since this background produces equal rates of same-flavor (SF) ee and $\mu\mu$ lepton pairs as opposite-flavor (OF) $e\mu$ lepton pairs, the OF yield can be used to estimate the SF yield, after correcting for the different electron vs. muon offline selection efficiencies and the different efficiencies for the ee , $\mu\mu$, and $e\mu$ triggers.

An important quantity needed to translate from the OF yield to a prediction for the background in the SF final state is the ratio $R_{\mu e} = \epsilon_\mu / \epsilon_e$, where ϵ_μ (ϵ_e) indicates the offline muon (electron) selection efficiency. This quantity can be extracted from data using the observed $Z \rightarrow \mu\mu$ and $Z \rightarrow ee$ yields in the preselection region, after correcting for the different trigger efficiencies.

Hence we define:

- $N_{ee}^{\text{trig}} = \epsilon_{ee}^{\text{trig}} N_{ee}^{\text{offline}}$,
- $N_{\mu\mu}^{\text{trig}} = \epsilon_{\mu\mu}^{\text{trig}} N_{\mu\mu}^{\text{offline}}$,
- $N_{e\mu}^{\text{trig}} = \epsilon_{e\mu}^{\text{trig}} N_{e\mu}^{\text{offline}}$.

Here $N_{\ell\ell}^{\text{trig}}$ denotes the number of selected Z events in the $\ell\ell$ channel passing the offline and trigger selection (in other words, the number of recorded and selected events), $\epsilon_{\ell\ell}^{\text{trig}}$ is the trigger efficiency, and $N_{\ell\ell}^{\text{offline}}$ is the number of events that would have passed the offline selection if the trigger had an efficiency of 100%. Thus we calculate the quantity:

$$R_{\mu e} = \sqrt{\frac{N_{\mu\mu}^{\text{offline}}}{N_{ee}^{\text{offline}}}} = \sqrt{\frac{N_{\mu\mu}^{\text{trig}} / \epsilon_{\mu\mu}^{\text{trig}}}{N_{ee}^{\text{trig}} / \epsilon_{ee}^{\text{trig}}}} = \sqrt{\frac{234132/0.86}{185555/0.95}} = 1.18 \pm 0.07. \quad (2)$$

Here we have used the $Z \rightarrow \mu\mu$ and $Z \rightarrow ee$ yields from Table 5 and the trigger efficiencies quoted in Sec. 3. The indicated uncertainty is due to the 3% uncertainties in the trigger efficiencies. The predicted yields in the ee and $\mu\mu$ final states are calculated from the observed $e\mu$ yield as

- $N_{ee}^{\text{predicted}} = \frac{N_{e\mu}^{\text{trig}}}{\epsilon_{e\mu}^{\text{trig}}} \frac{\epsilon_{ee}^{\text{trig}}}{2R_{\mu e}} = \frac{N_{e\mu}^{\text{trig}}}{0.93} \frac{0.95}{2 \times 1.18} = (0.43 \pm 0.05) \times N_{e\mu}^{\text{trig}}$,
- $N_{\mu\mu}^{\text{predicted}} = \frac{N_{e\mu}^{\text{trig}}}{\epsilon_{e\mu}^{\text{trig}}} \frac{\epsilon_{\mu\mu}^{\text{trig}} R_{\mu e}}{2} = \frac{N_{e\mu}^{\text{trig}}}{0.95} \frac{0.86 \times 1.18}{2} = (0.53 \pm 0.07) \times N_{e\mu}^{\text{trig}}$,

and the predicted yield in the combined ee and $\mu\mu$ channel is simply the sum of these two predictions:

- $N_{ee+\mu\mu}^{\text{predicted}} = (0.97 \pm 0.06) \times N_{e\mu}^{\text{trig}}$.

Note that the relative uncertainty in the combined ee and $\mu\mu$ prediction is smaller than those for the individual ee and $\mu\mu$ predictions because the uncertainty in $R_{\mu e}$ cancels when summing the ee and $\mu\mu$ predictions.

To improve the statistical precision of the FS background estimate, we remove the requirement that the $e\mu$ lepton pair falls in the Z mass window. Instead we scale the $e\mu$ yield by K , the efficiency for $e\mu$ events to satisfy the Z mass requirement, extracted from simulation. In Fig. 6 we display the value of K in data and simulation, for a variety of E_T^{miss} requirements, for the inclusive analysis. Based on this we chose $K = 0.14 \pm 0.02$ for the lower E_T^{miss} regions, $K = 0.14 \pm 0.04$ for the $E_T^{\text{miss}} > 200$ GeV region, and $K = 0.14 \pm 0.08$ for $E_T^{\text{miss}} > 300$ GeV, where the larger uncertainties reflect the reduced statistical precision at large E_T^{miss} . The corresponding plot for the targeted analysis, including the b-veto, is displayed in Fig. 7. Based on this we chose $K = 0.13 \pm 0.02$ for all E_T^{miss} regions up to $E_T^{\text{miss}} > 100$ GeV. For the $E_T^{\text{miss}} > 150$ GeV region we choose $K = 0.13 \pm 0.03$ and for the $E_T^{\text{miss}} > 200$ GeV region we choose $K = 0.13 \pm 0.05$, due to the reduced statistical precision.

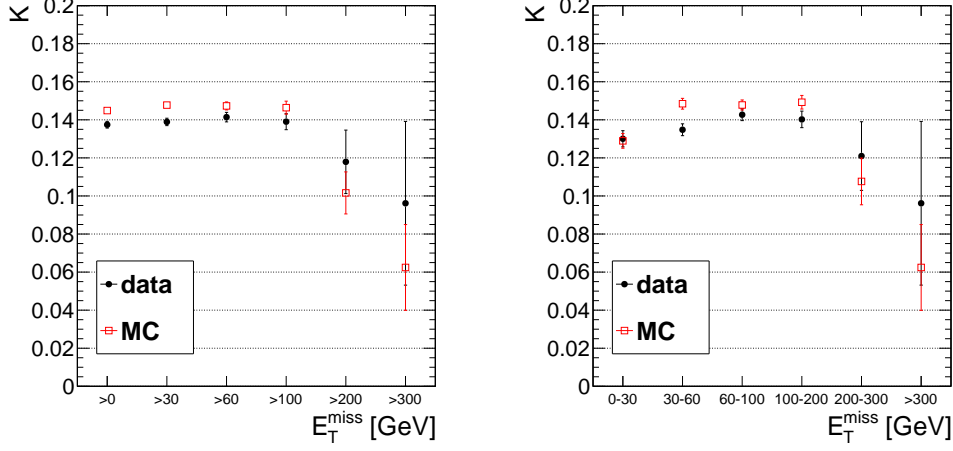


Figure 6: The efficiency for $e\mu$ events to satisfy the dilepton mass requirement, K , in data and simulation for inclusive E_T^{miss} intervals (left) and exclusive E_T^{miss} intervals (right) for the inclusive analysis. Based on this we chose $K = 0.14 \pm 0.02$ for the lower E_T^{miss} regions, $K = 0.14 \pm 0.04$ for the $E_T^{\text{miss}} > 200$ GeV region, and $K = 0.14 \pm 0.08$ for $E_T^{\text{miss}} > 300$ GeV.

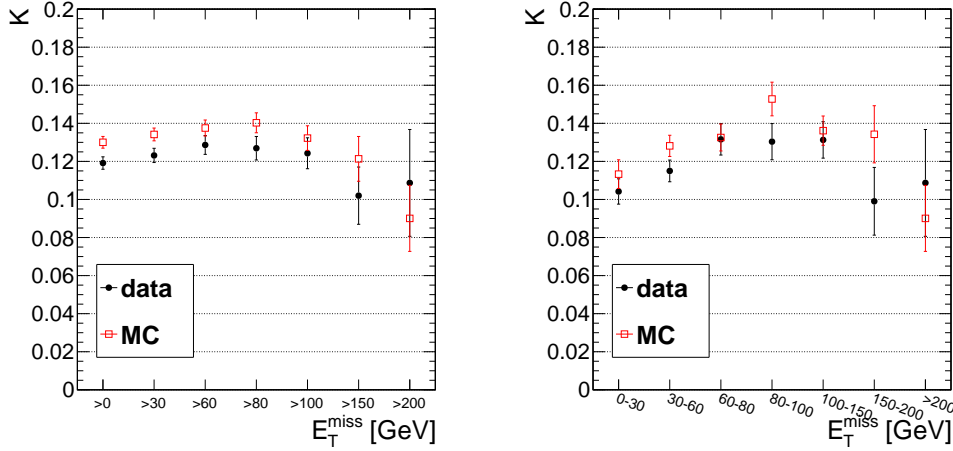


Figure 7: The efficiency for $e\mu$ events to satisfy the dilepton mass requirement, K , in data and simulation for inclusive E_T^{miss} intervals (left) and exclusive E_T^{miss} intervals (right) for the targeted analysis, including the b-veto. Based on this we chose $K = 0.13 \pm 0.02$ for the E_T^{miss} regions up to $E_T^{\text{miss}} > 100$ GeV. For $E_T^{\text{miss}} > 150$ we choose $K = 0.13 \pm 0.03$, for $E_T^{\text{miss}} > 200$ GeV we choose $K = 0.13 \pm 0.05$.

6.3 Estimating the WZ and ZZ Background with MC

Backgrounds from $W(\ell\nu)Z(\ell\ell)$ where the W lepton is not identified or is outside acceptance, and $Z(\nu\nu)Z(\ell\ell)$, are estimated from simulation. The MC modeling of these processes is validated by comparing the MC predictions with data in control samples with exactly 3 leptons (WZ control sample) and exactly 4 leptons (ZZ control sample). The critical samples are the WZJetsTo3LNu and ZZJetsTo4L, listed in Table 1 (the WZJetsTo2L2Q, ZZJetsTo2L2Q, and ZZJetsTo2L2Nu samples are also used in this analysis but their contribution to the 3-lepton and 4-lepton control samples is negligible).

6.3.1 WZ Validation Studies

A pure WZ sample can be selected in data with the requirements:

- Exactly 3 $p_T > 20$ GeV leptons passing analysis identification and isolation requirements,
- 2 of the 3 leptons must fall in the Z window 81-101 GeV,
- $E_T^{\text{miss}} > 50$ GeV (to suppress DY).

The data and MC yields passing the above selection are in Table 7. The inclusive yields (without any jet requirements) agree within 16%, which is consistent within the $\approx 15\%$ uncertainty in the theory prediction for the WZ cross section. A data vs. MC comparison of kinematic distributions (jet multiplicity, E_T^{miss} , Z p_T) is given in Fig. 8. High E_T^{miss} values in WZ and ZZ events arise from highly boosted W or Z bosons that decay leptonically, and we therefore check that the MC does a reasonable job of reproducing the p_T distributions of the leptonically decaying Z. While the inclusive WZ yields are in reasonable agreement, we observe an excess in data in events with at least 2 jets, corresponding to the jet multiplicity requirement in our preselection. We observe 200 events in data while the MC predicts 130 ± 3.1 (stat), representing an excess of 53%, as indicated in Table 8, and we therefore assess an uncertainty of 50% on the WZ background.

Table 7: Data and Monte Carlo yields passing the WZ preselection.

Sample	ee	$\mu\mu$	$e\mu$	total
WZ	244.9 ± 1.6	317.9 ± 1.8	17.0 ± 0.4	579.7 ± 2.4
Z + jets	2.5 ± 2.0	6.4 ± 3.9	0.0 ± 0.0	8.9 ± 4.3
ZZ	5.3 ± 0.0	7.1 ± 0.1	0.4 ± 0.0	12.8 ± 0.1
$t\bar{t}$	2.5 ± 1.3	6.7 ± 2.0	7.5 ± 2.1	16.7 ± 3.2
single top	0.0 ± 0.0	0.5 ± 0.5	0.0 ± 0.0	0.5 ± 0.5
WW	0.0 ± 0.0	0.1 ± 0.1	0.2 ± 0.1	0.3 ± 0.1
ttV	8.6 ± 0.4	10.3 ± 0.4	2.5 ± 0.2	21.5 ± 0.7
VVV	3.4 ± 0.1	4.3 ± 0.1	0.6 ± 0.1	8.3 ± 0.2
tot SM MC	267.1 ± 2.9	353.3 ± 4.7	28.2 ± 2.2	648.6 ± 6.0
data	312	391	50	753

Table 8: Data and Monte Carlo yields passing the WZ preselection and $N_{\text{jets}} \geq 2$.

Sample	ee	$\mu\mu$	$e\mu$	total
$t\bar{t}$	1.6 ± 0.9	3.4 ± 1.5	1.8 ± 1.1	6.9 ± 2.0
Z + jets	1.9 ± 1.9	0.0 ± 0.0	0.0 ± 0.0	1.9 ± 1.9
WZ	40.0 ± 0.7	51.5 ± 0.7	2.7 ± 0.2	94.3 ± 1.0
ZZ	1.0 ± 0.0	1.4 ± 0.0	0.1 ± 0.0	2.6 ± 0.0
single top	0.0 ± 0.0	0.5 ± 0.5	0.0 ± 0.0	0.5 ± 0.5
WW	0.0 ± 0.0	0.0 ± 0.0	0.0 ± 0.0	0.0 ± 0.0
ttV	8.0 ± 0.4	9.5 ± 0.4	2.2 ± 0.2	19.6 ± 0.6
VVV	1.9 ± 0.1	2.6 ± 0.1	0.2 ± 0.0	4.6 ± 0.2
tot SM MC	54.4 ± 2.2	69.0 ± 1.8	6.9 ± 1.1	130.4 ± 3.1
data	87	91	22	200

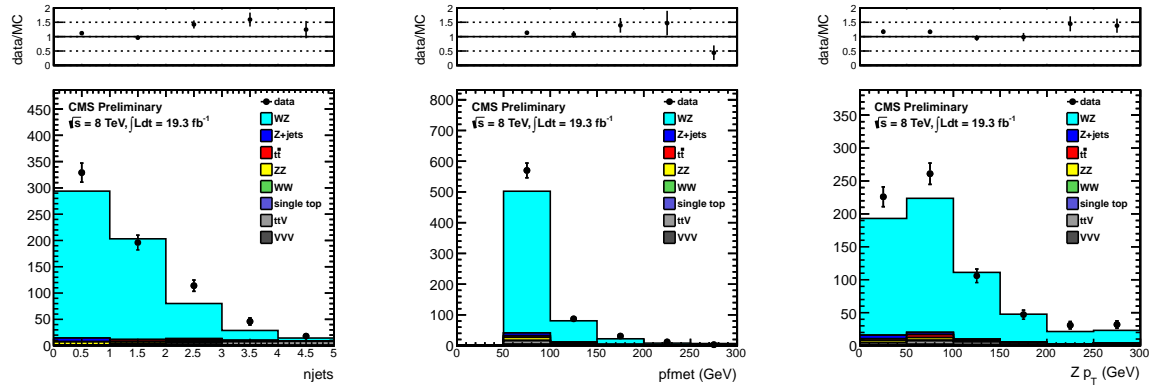


Figure 8: Data vs. MC comparisons for the WZ selection discussed in the text for 19.5 fb^{-1} . The number of jets, missing transverse energy, and Z boson transverse momentum are displayed.

6.3.2 ZZ Validation Studies

A pure ZZ sample can be selected in data with the requirements:

- Exactly 4 $p_T > 20$ GeV leptons passing analysis identification and isolation requirements,
- 2 of the 4 leptons must fall in the Z window 81-101 GeV.

The data and MC yields passing the above selection are in Table 9. In this ZZ-dominated sample we observe good agreement between the data yield and the MC prediction. After requiring 2 jets (corresponding to the requirement in the analysis selection), we observe 14 events in data and the MC predicts 13.2 ± 0.2 events. Due to the limited statistical precision we assign an uncertainty of 50% on the ZZ yield.

Table 9: Data and Monte Carlo yields for the ZZ preselection.

Sample	ee	$\mu\mu$	$e\mu$	total
ZZ	52.7 ± 0.2	73.3 ± 0.2	3.4 ± 0.0	129.4 ± 0.3
WZ	0.1 ± 0.0	0.1 ± 0.0	0.0 ± 0.0	0.3 ± 0.1
Z + jets	0.0 ± 0.0	0.0 ± 0.0	0.0 ± 0.0	0.0 ± 0.0
$t\bar{t}$	0.0 ± 0.0	0.0 ± 0.0	0.0 ± 0.0	0.0 ± 0.0
WW	0.0 ± 0.0	0.0 ± 0.0	0.0 ± 0.0	0.0 ± 0.0
single top	0.0 ± 0.0	0.0 ± 0.0	0.0 ± 0.0	0.0 ± 0.0
ttV	1.3 ± 0.2	1.4 ± 0.2	0.3 ± 0.1	3.0 ± 0.2
VVV	0.6 ± 0.1	0.8 ± 0.1	0.0 ± 0.0	1.4 ± 0.1
tot SM MC	54.7 ± 0.3	75.6 ± 0.3	3.8 ± 0.1	134.1 ± 0.4
data	56	80	5	141

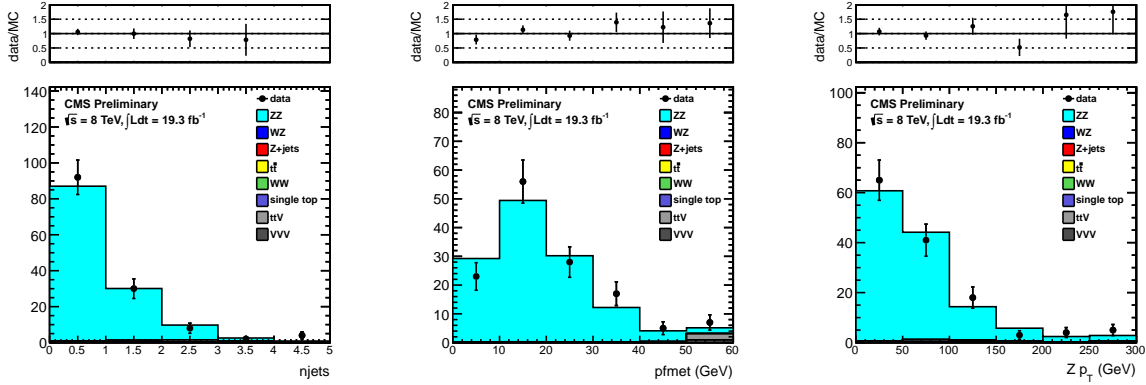


Figure 9: Data vs. MC comparisons for the ZZ selection discussed in the text for 19.5 fb^{-1} . The number of jets, missing transverse energy, and Z boson transverse momentum are displayed.

7 Results

In this section we provide the results of the inclusive and targeted searches. The observed and predicted E_T^{miss} distributions for the inclusive analysis are indicated in Fig. 10. A summary of the results in the signal regions is provided in Table 10. Good agreement is observed between the data and the predicted background over the full E_T^{miss} range. The separate results for the ee and $\mu\mu$ channels are presented in App. A.

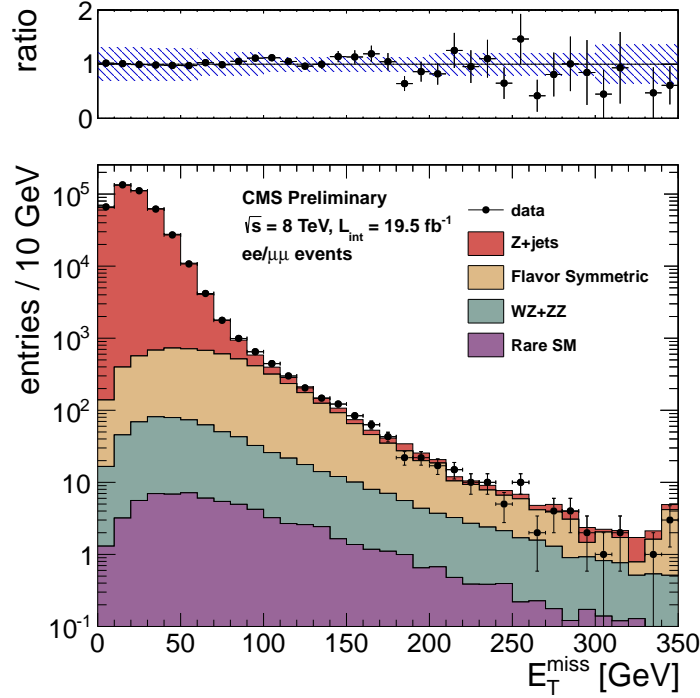


Figure 10: Results of the inclusive analysis. The observed E_T^{miss} distribution (black points) is compared with the sum of the predicted E_T^{miss} distributions from Z + jets, flavor-symmetric backgrounds, and WZ+ZZ backgrounds. The ratio of observed to predicted yields in each bin is indicated. The error bars indicate the statistical uncertainty in the data and the shaded band indicates the total background uncertainty.

Table 10: Summary of results in the inclusive analysis. The total background is the sum of the Z + jets background predicted from the E_T^{miss} templates method (Z + jets bkg), the flavor-symmetric background predicted from $e\mu$ events (FS bkg), and the WZ and ZZ backgrounds predicted from MC (WZ bkg and ZZ bkg). All uncertainties include both the statistical and systematic components. The Gaussian significance of the deviation between the data and total background is indicated for signal regions with at least 20 observed events.

	E_T^{miss} 0–30 GeV	E_T^{miss} 30–60 GeV	E_T^{miss} 60–100 GeV	E_T^{miss} 100–200 GeV	E_T^{miss} 200–300 GeV	E_T^{miss} > 300 GeV
Z + jets bkg	308067 ± 92421	99280 ± 29785	5155 ± 1547	238 ± 72	11.6 ± 3.6	2.8 ± 1.0
FS bkg	972 ± 151	1889 ± 293	2022 ± 314	1011 ± 157	50.7 ± 15.0	7.2 ± 4.3
WZ bkg	108.9 ± 54.5	186.4 ± 93.2	137.7 ± 68.9	78.7 ± 39.3	11.1 ± 5.6	3.1 ± 3.1
ZZ bkg	12.1 ± 6.1	26.6 ± 13.3	29.8 ± 14.9	29.8 ± 14.9	6.2 ± 3.1	2.0 ± 2.0
Rare SM bkg	10.1 ± 5.1	21.0 ± 10.5	20.6 ± 10.3	17.9 ± 9.0	3.2 ± 1.6	1.1 ± 1.1
Total background	309170 ± 92421	101403 ± 29786	7365 ± 1580	1375 ± 178	82.8 ± 16.8	16.2 ± 5.8
Data	311030	99543	7578	1450	79	7

272 The observed and predicted E_T^{miss} distributions for the targeted analysis are indicated in Fig. 11. A summary of
 273 the results in the signal regions is provided in Table 11. Good agreement is observed between the data and the
 274 predicted background over the full E_T^{miss} range. The separate results for the ee and $\mu\mu$ channels are presented in
 275 App. A.

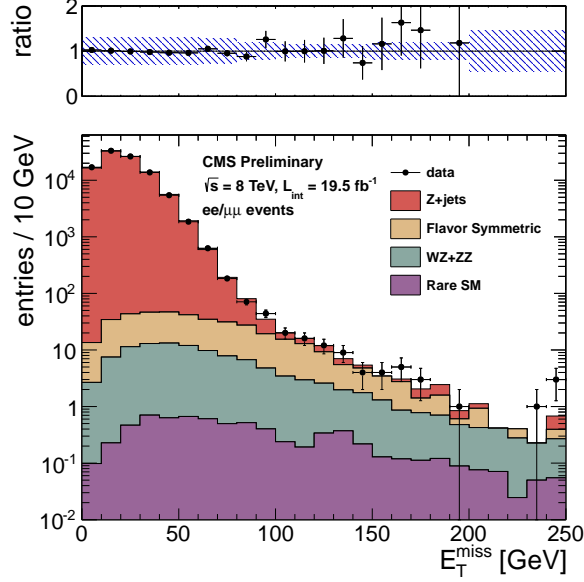


Figure 11: Results of the Z + dijet analysis. The observed E_T^{miss} distribution (black points) is compared with the sum of the predicted E_T^{miss} distributions from Z + jets, flavor-symmetric (FS), sum of WZ and ZZ (WZ+ZZ), and rare SM backgrounds. The ratio of observed to predicted yields in each bin is indicated. The error bars indicate the statistical uncertainty in the data and the shaded band indicates the total background uncertainty.

Table 11: Summary of results in the targeted analysis. The total background is the sum of the Z + jets background predicted from the E_T^{miss} templates method (Z + jets bkg), the flavor-symmetric background predicted from $e\mu$ events (FS bkg), and the WZ and ZZ backgrounds predicted from MC (WZ bkg and ZZ bkg). All uncertainties include both the statistical and systematic components. The Gaussian significance of the deviation between the data and total background is indicated for signal regions with at least 20 observed events.

	E_T^{miss} 0–30 GeV	E_T^{miss} 30–60 GeV	E_T^{miss} 60–80 GeV	E_T^{miss} 80–100 GeV
Z + jets bkg	75652 ± 22696	21414 ± 6425	722 ± 217	68.9 ± 21.2
FS bkg	69.9 ± 11.9	96.7 ± 16.3	48.3 ± 8.3	35.2 ± 6.2
WZ bkg	17.7 ± 8.8	29.8 ± 14.9	13.0 ± 6.5	7.4 ± 3.7
ZZ bkg	3.1 ± 1.5	6.4 ± 3.2	3.5 ± 1.8	3.2 ± 1.6
Rare SM bkg	0.8 ± 0.4	2.0 ± 1.0	1.1 ± 0.6	0.9 ± 0.5
Total background	75744 ± 22696	21549 ± 6425	788 ± 218	116 ± 22
Data	76302	20991	809	115
	E_T^{miss} 100–120 GeV	E_T^{miss} 120–150 GeV	E_T^{miss} 150–200 GeV	E_T^{miss} > 200 GeV
Z + jets bkg	7.8 ± 2.5	4.8 ± 1.5	2.1 ± 0.7	0.5 ± 0.1
FS bkg	21.9 ± 4.0	13.2 ± 2.5	5.7 ± 1.6	0.8 ± 0.4
WZ bkg	4.0 ± 2.0	3.3 ± 1.6	2.0 ± 1.0	0.9 ± 0.9
ZZ bkg	1.9 ± 1.0	2.1 ± 1.1	1.5 ± 0.8	1.4 ± 1.4
Rare SM bkg	0.4 ± 0.2	0.9 ± 0.5	0.6 ± 0.3	0.4 ± 0.4
Total background	36.1 ± 5.2	24.3 ± 3.6	11.8 ± 2.2	3.9 ± 1.8
Data	36	25	13	4

8 Summary

This note presents a search for BSM physics in final states with leptonically-decaying Z bosons, jets, and E_T^{miss} . Two strategies were pursued. The first is an inclusive approach which targets BSM scenarios with Z bosons produced in the decays of strongly-interacting particles. The second is a targeted approach which focuses on BSM scenarios where the Z bosons are produced in the decays of weakly-interacting particles. The main backgrounds are estimated with data-driven techniques. Good agreement is observed between the data and the predicted backgrounds over the full E_T^{miss} range, for both searches.

References

- [1] CMS Collaboration, “Search for physics beyond the standard model in events with a Z boson, jets, and missing transverse energy in pp collisions at $\sqrt{s} = 7$ TeV,” arXiv:1204.3774v1 [hep-ex].
- [2] SUS-12-006, paper draft
- [3] <https://twiki.cern.ch/twiki/bin/viewauth/CMS/EgammaCutBasedIdentification>
- [4] <https://twiki.cern.ch/twiki/bin/viewauth/CMS/EgammaEARhoCorrection>
- [5] <https://twiki.cern.ch/twiki/bin/view/CMSPublic/SWGuideMuonId>
- [6] M. Chen, AN 2012/237 “Interpretation of the Same-Sign di-leptons with bjets and MET search”

A Results in the ee and $\mu\mu$ Channels

In this section we provide the results of the inclusive and targeted searches, separately in the ee and $\mu\mu$ channels. The E_T^{miss} distributions in the inclusive analysis for the ee channel are displayed in Fig. 12 and the signal region yields are presented in Table 12. The E_T^{miss} distributions in the inclusive analysis for the $\mu\mu$ channel are displayed in Fig. 13 and the signal region yields are presented in Table 13.

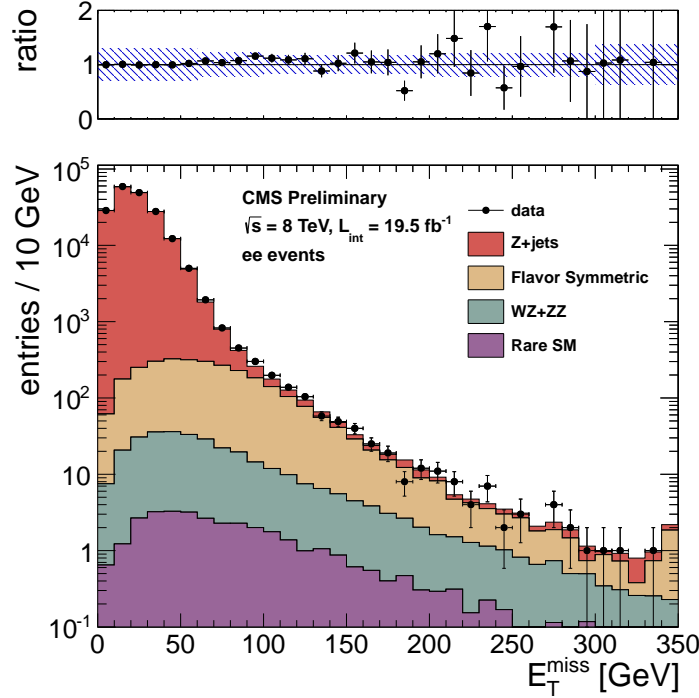


Figure 12: Results of the inclusive analysis in the ee channel. The observed E_T^{miss} distribution (black points) is compared with the sum of the predicted E_T^{miss} distributions from Z + jets , flavor-symmetric backgrounds, and WZ+ZZ backgrounds. The ratio of observed to predicted yields in each bin is indicated. The error bars indicate the statistical uncertainty in the data and the shaded band indicates the total background uncertainty.

Table 12: Summary of results in the inclusive analysis in the ee channel. The total background is the sum of the Z + jets background predicted from the E_T^{miss} templates method (Z + jets bkg), the flavor-symmetric background predicted from $e\mu$ events (FS bkg), and the WZ and ZZ backgrounds predicted from MC (WZ bkg and ZZ bkg). All uncertainties include both the statistical and systematic components. The Gaussian significance of the deviation between the data and total background is indicated for signal regions with at least 20 observed events.

	E_T^{miss} 0–30 GeV	E_T^{miss} 30–60 GeV	E_T^{miss} 60–100 GeV	E_T^{miss} 100–200 GeV	E_T^{miss} 200–300 GeV	E_T^{miss} > 300 GeV
Z + jets bkg	135952 ± 40791	43966 ± 13198	2302 ± 699	107 ± 55	5.2 ± 1.6	1.3 ± 0.4
FS bkg	431 ± 81	838 ± 156	896 ± 167	448 ± 84	22.5 ± 7.1	3.2 ± 1.9
WZ bkg	49.0 ± 24.5	83.6 ± 41.8	62.6 ± 31.3	35.7 ± 17.9	5.2 ± 2.6	1.5 ± 1.5
ZZ bkg	5.3 ± 2.7	11.9 ± 6.0	13.2 ± 6.6	13.3 ± 6.7	3.0 ± 1.5	0.9 ± 0.9
rare SM bkg	4.5 ± 2.3	9.7 ± 4.9	9.2 ± 4.6	8.4 ± 4.2	1.7 ± 0.8	0.5 ± 0.5
total bkg	136442 ± 40791	44909 ± 13199	3283 ± 719	613 ± 102	37.5 ± 7.9	7.4 ± 2.7
data	136404	44947	3508	651	42	3

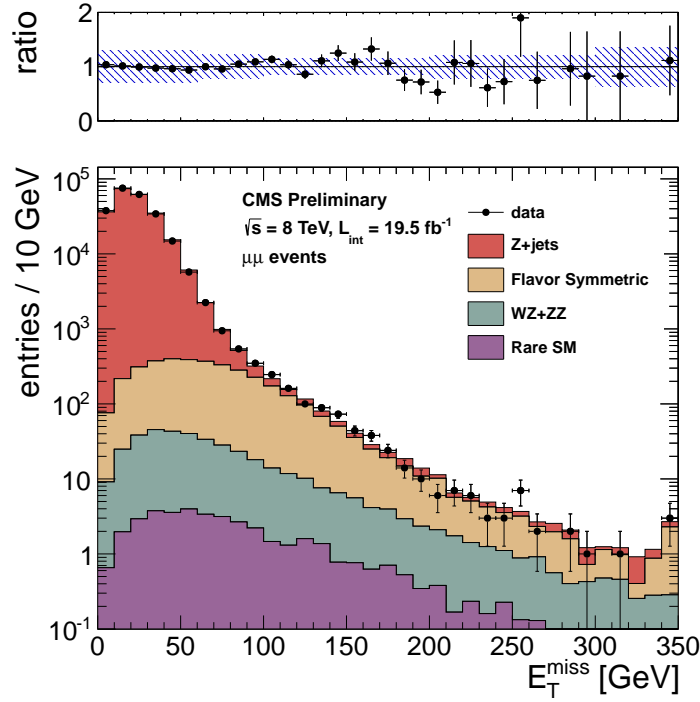


Figure 13: Results of the inclusive analysis in the $\mu\mu$ channel. The observed E_T^{miss} distribution (black points) is compared with the sum of the predicted E_T^{miss} distributions from Z + jets , flavor-symmetric backgrounds, and WZ+ZZ backgrounds. The ratio of observed to predicted yields in each bin is indicated. The error bars indicate the statistical uncertainty in the data and the shaded band indicates the total background uncertainty.

Table 13: Summary of results in the inclusive analysis in the $\mu\mu$ channel. The total background is the sum of the Z + jets background predicted from the E_T^{miss} templates method (Z + jets bkg), the flavor-symmetric background predicted from $e\mu$ events (FS bkg), and the WZ and ZZ backgrounds predicted from MC (WZ bkg and ZZ bkg). All uncertainties include both the statistical and systematic components. The Gaussian significance of the deviation between the data and total background is indicated for signal regions with at least 20 observed events.

	E_T^{miss} 0–30 GeV	E_T^{miss} 30–60 GeV	E_T^{miss} 60–100 GeV	E_T^{miss} 100–200 GeV	E_T^{miss} 200–300 GeV	E_T^{miss} > 300 GeV
Z + jets bkg	172129 ± 51640	55328 ± 16600	2854 ± 858	130 ± 45	6.3 ± 2.0	1.5 ± 0.5
FS bkg	531 ± 99	1032 ± 193	1105 ± 206	553 ± 103	27.7 ± 8.7	3.9 ± 2.4
WZ bkg	59.9 ± 30.0	102.8 ± 51.4	75.1 ± 37.6	43.0 ± 21.5	5.9 ± 3.0	1.6 ± 1.6
ZZ bkg	6.8 ± 3.4	14.7 ± 7.4	16.6 ± 8.3	16.5 ± 8.3	3.3 ± 1.6	1.1 ± 1.1
rare SM bkg	5.6 ± 2.8	11.3 ± 5.7	11.4 ± 5.7	9.5 ± 4.8	1.6 ± 0.8	0.6 ± 0.6
total bkg	172733 ± 51640	56489 ± 16602	4062 ± 884	752 ± 115	44.8 ± 9.6	8.8 ± 3.2
data	174626	54596	4070	799	37	4

296 The E_T^{miss} distributions in the targeted analysis for the ee channel are displayed in Fig. 14 and the signal region
 297 yields are presented in Table 14. The E_T^{miss} distributions in the inclusive analysis for the $\mu\mu$ channel are displayed
 298 in Fig. 15 and the signal region yields are presented in Table 15.

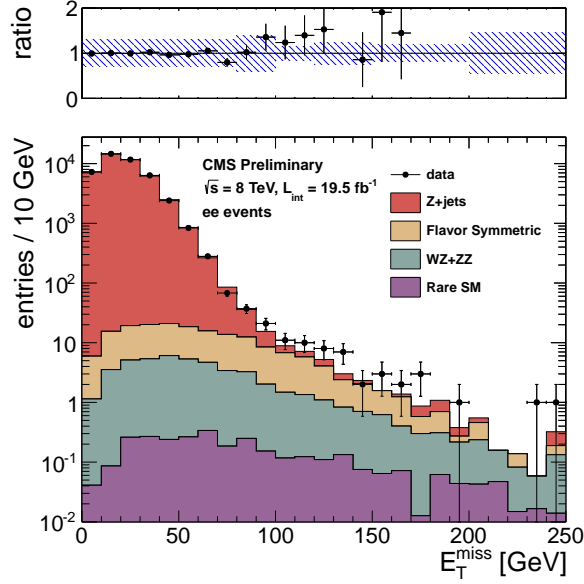


Figure 14: Results of the targeted analysis in the ee channel. The observed E_T^{miss} distribution (black points) is compared with the sum of the predicted E_T^{miss} distributions from Z + jets , flavor-symmetric backgrounds, and WZ+ZZ backgrounds. The ratio of observed to predicted yields in each bin is indicated. The error bars indicate the statistical uncertainty in the data and the shaded band indicates the total background uncertainty.

Table 14: Summary of results in the targeted analysis in the ee channel. The total background is the sum of the Z + jets background predicted from the E_T^{miss} templates method (Z + jets bkg), the flavor-symmetric background predicted from $e\mu$ events (FS bkg), and the WZ and ZZ backgrounds predicted from MC (WZ bkg and ZZ bkg). All uncertainties include both the statistical and systematic components. The Gaussian significance of the deviation between the data and total background is indicated for signal regions with at least 20 observed events.

	E_T^{miss} 0–30 GeV	E_T^{miss} 30–60 GeV	E_T^{miss} 60–80 GeV	E_T^{miss} 80–100 GeV
Z + jets bkg	33409 ± 10031	9480 ± 2855	321 ± 105	30.8 ± 20.4
FS bkg	31.0 ± 6.2	42.9 ± 8.5	21.4 ± 4.3	15.6 ± 3.2
WZ bkg	8.0 ± 4.0	13.1 ± 6.6	6.0 ± 3.0	3.5 ± 1.7
ZZ bkg	1.4 ± 0.7	2.9 ± 1.5	1.5 ± 0.8	1.4 ± 0.7
Rare SM bkg	0.4 ± 0.2	0.8 ± 0.4	0.5 ± 0.3	0.4 ± 0.2
total bkg	33450 ± 10031	9540 ± 2855	350 ± 106	51.7 ± 20.7
data	33420	9570	347	58
	E_T^{miss} 100–120 GeV	E_T^{miss} 120–150 GeV	E_T^{miss} 150–200 GeV	E_T^{miss} > 200 GeV
Z + jets bkg	3.5 ± 1.1	2.1 ± 2.1	0.9 ± 0.3	0.2 ± 0.1
FS bkg	9.7 ± 2.0	5.9 ± 1.3	2.5 ± 0.8	0.3 ± 0.2
WZ bkg	1.7 ± 0.9	1.5 ± 0.8	0.9 ± 0.4	0.4 ± 0.4
ZZ bkg	0.8 ± 0.4	0.8 ± 0.4	0.7 ± 0.4	0.7 ± 0.7
rare SM bkg	0.2 ± 0.1	0.3 ± 0.2	0.3 ± 0.1	0.2 ± 0.2
total bkg	16.1 ± 2.5	10.6 ± 2.6	5.3 ± 1.0	1.8 ± 0.8
data	21	17	9	2

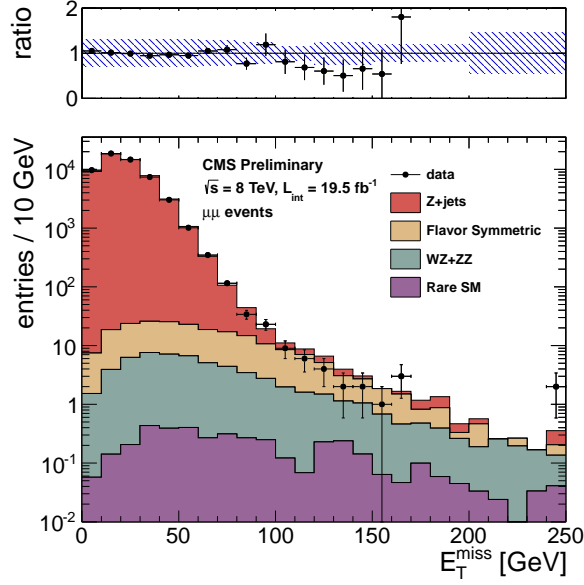


Figure 15: Results of the targeted analysis in the $\mu\mu$ channel. The observed E_T^{miss} distribution (black points) is compared with the sum of the predicted E_T^{miss} distributions from Z + jets, flavor-symmetric backgrounds, and WZ+ZZ backgrounds. The ratio of observed to predicted yields in each bin is indicated. The error bars indicate the statistical uncertainty in the data and the shaded band indicates the total background uncertainty.

Table 15: Summary of results in the targeted analysis in the $\mu\mu$ channel. The total background is the sum of the Z + jets background predicted from the E_T^{miss} templates method (Z + jets bkg), the flavor-symmetric background predicted from $e\mu$ events (FS bkg), and the WZ and ZZ backgrounds predicted from MC (WZ bkg and ZZ bkg). All uncertainties include both the statistical and systematic components. The Gaussian significance of the deviation between the data and total background is indicated for signal regions with at least 20 observed events.

	E_T^{miss} 0–30 GeV	E_T^{miss} 30–60 GeV	E_T^{miss} 60–80 GeV	E_T^{miss} 80–100 GeV
Z + jets bkg	42245 ± 12675	11934 ± 3583	401 ± 122	38.1 ± 14.2
FS bkg	38.2 ± 7.6	52.8 ± 10.5	26.4 ± 5.3	19.2 ± 3.9
WZ bkg	9.7 ± 4.8	16.7 ± 8.3	6.9 ± 3.5	3.9 ± 2.0
ZZ bkg	1.7 ± 0.8	3.5 ± 1.8	2.0 ± 1.0	1.8 ± 0.9
rare SM bkg	0.4 ± 0.2	1.2 ± 0.6	0.6 ± 0.3	0.5 ± 0.3
total bkg	42295 ± 12675	12008 ± 3583	437 ± 123	63.6 ± 14.9
data	42882	11421	462	57
	E_T^{miss} 100–120 GeV	E_T^{miss} 120–150 GeV	E_T^{miss} 150–200 GeV	E_T^{miss} > 200 GeV
Z + jets bkg	4.3 ± 1.4	2.7 ± 2.7	1.1 ± 0.4	0.3 ± 0.1
FS bkg	12.0 ± 2.5	7.2 ± 1.6	3.1 ± 0.9	0.4 ± 0.2
WZ bkg	2.3 ± 1.2	1.7 ± 0.9	1.1 ± 0.6	0.5 ± 0.5
ZZ bkg	1.1 ± 0.6	1.3 ± 0.7	0.8 ± 0.4	0.7 ± 0.7
rare SM bkg	0.2 ± 0.1	0.6 ± 0.3	0.3 ± 0.2	0.2 ± 0.2
total bkg	19.9 ± 3.1	13.6 ± 3.3	6.5 ± 1.2	2.1 ± 1.0
data	15	8	4	2

299 **B** E_T^{miss} Templates from $\gamma + \text{jets}$ Sample

300 In this section we display the templates used for the inclusive analysis (red) and the targeted analysis (blue).

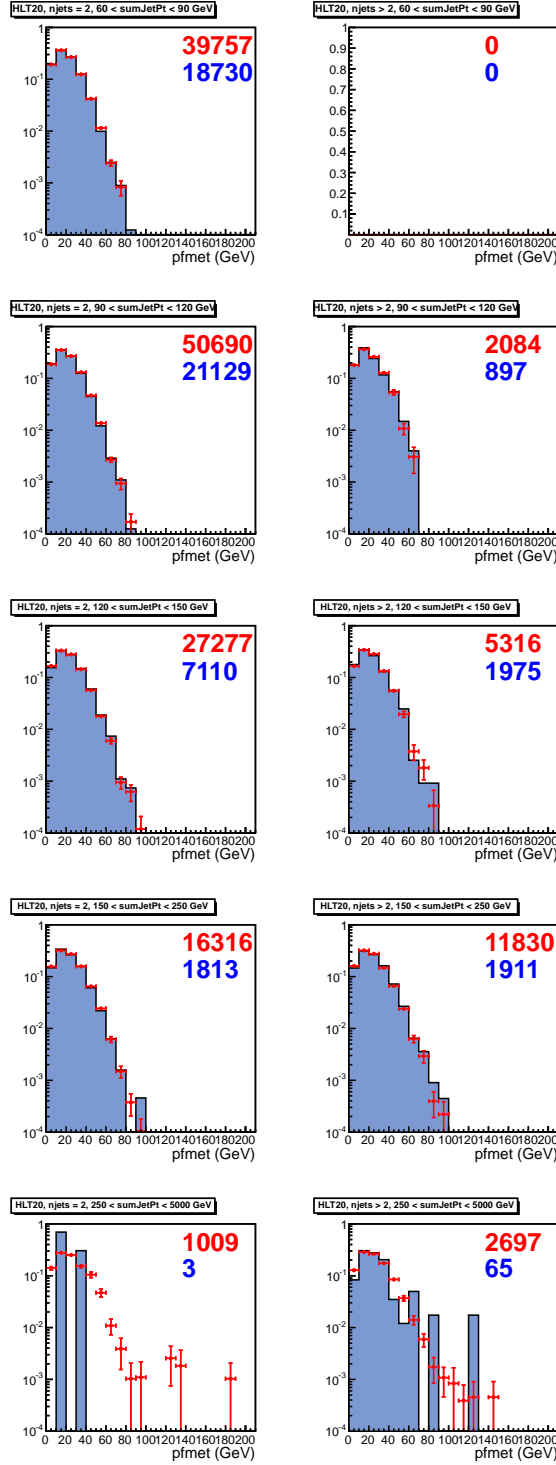


Figure 16: E_T^{miss} templates collected with the $p_T > 22$ GeV single photon trigger. The number in red (blue) indicates the number of entries in the template for the inclusive (targeted) analysis.

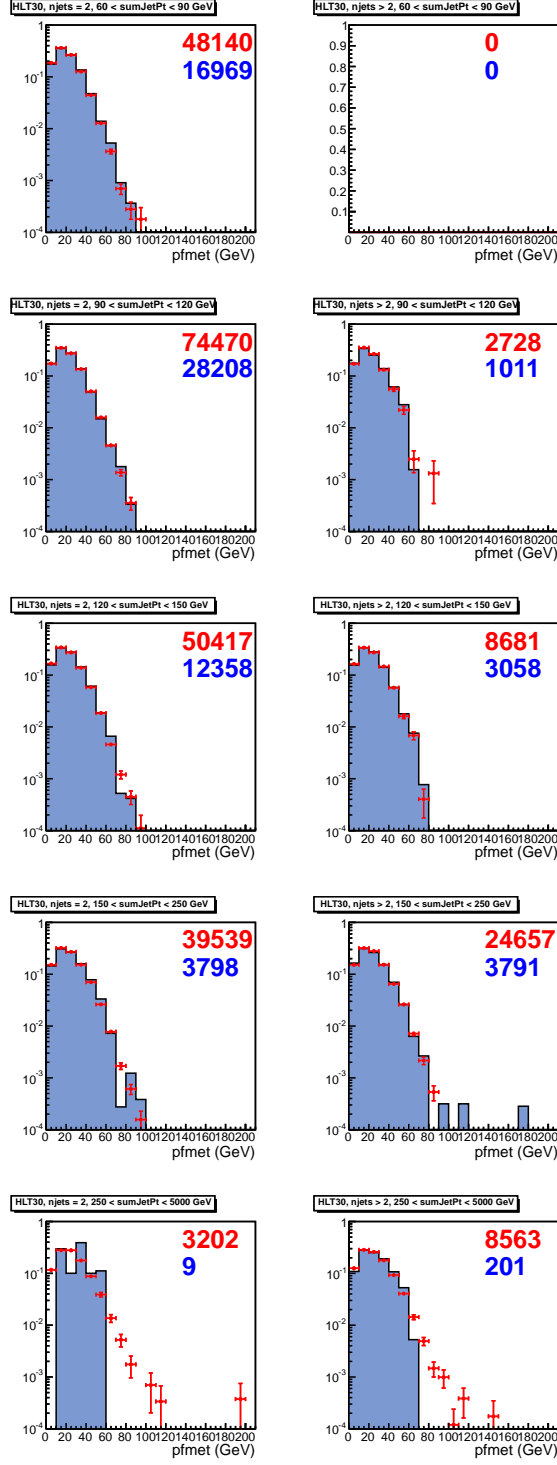


Figure 17: E_T^{miss} templates collected with the $p_T > 36$ GeV single photon trigger. The number in red (blue) indicates the number of entries in the template for the inclusive (targeted) analysis.

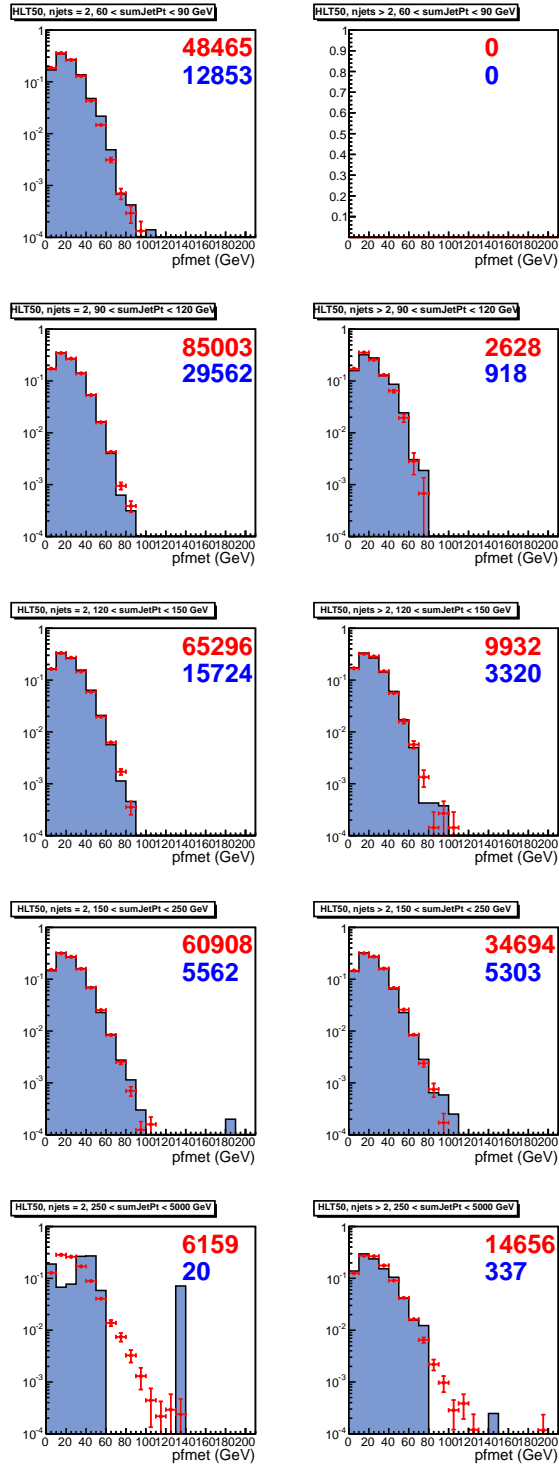


Figure 18: E_T^{miss} templates collected with the $p_T > 50$ GeV single photon trigger. The number in red (blue) indicates the number of entries in the template for the inclusive (targeted) analysis.

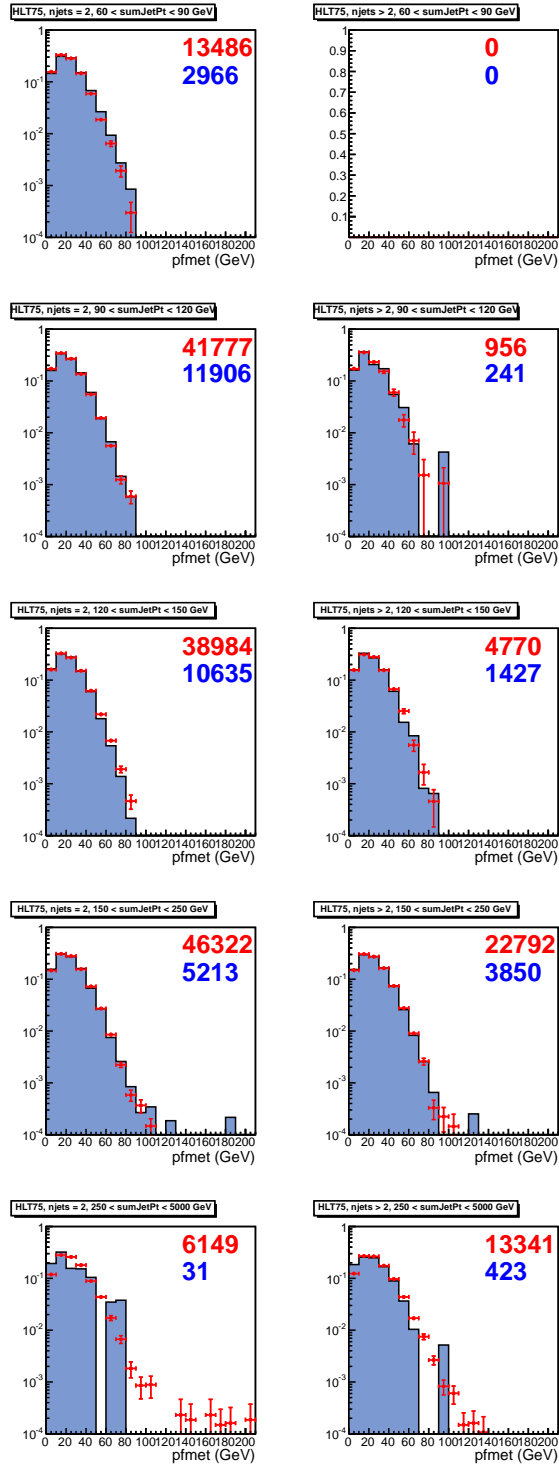


Figure 19: E_T^{miss} templates collected with the $p_T > 75$ GeV single photon trigger. The number in red (blue) indicates the number of entries in the template for the inclusive (targeted) analysis.

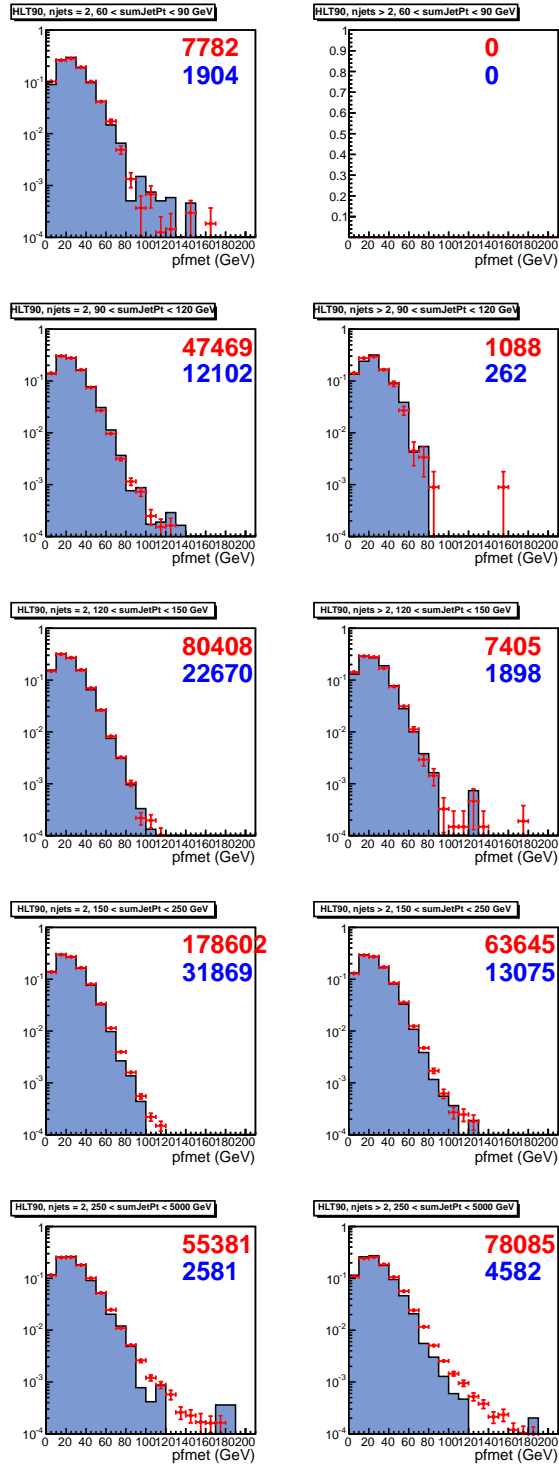


Figure 20: E_T^{miss} templates collected with the $p_T > 90$ GeV single photon trigger. The number in red (blue) indicates the number of entries in the template for the inclusive (targeted) analysis.